

The extraction of light cone parton distributions from lattice quantum chromodynamics

Savvas Zafeiropoulos
HadStruc Collaboration

CPT, Marseille

23.05.2023

ECT, Trento

In collaboration with P. Barry (JLAB), L. DelDebbio (Edinburgh), R. Edwards (JLAB), C. Egerer (JLAB), T. Giani (NIKHEF), B. Joo (ORNL), J. Karpie (JLAB), N. Karthik (APS), T. Khan (Brac U.), W. Melnitchouk (JLAB), K. Orginos (College of William & Mary and JLAB), A. Radyushkin (ODU and JLAB), D. Richards (JLAB), E. Romero (JLAB), A. Rothkopf (Stavanger U.), N. Sato (JLAB), R. Sufian (BNL)

PDFs are of paramount importance because...

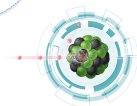
- The uncertainties in PDFs are the **dominant theoretical uncertainties** in Higgs couplings, α_s and the mass of the W boson
- Beyond the LHC, PDFs play an important role, for instance in astroparticle physics, such as for the accurate predictions for signal and background events at ultra-high energy neutrino telescopes (ANITA, IceCube, Pierre Auger Observatory)



Future Circular Collider
Circumference: 80-100 km
Energy: 100 TeV (pp)
>350 GeV (e^+e^-)

Large Hadron Collider
Circumference: 27 km
Energy: 14 TeV (pp)
209 GeV (e^+e^-)

Tevatron (closed)
Circumference: 6.2 km
Energy: 2 TeV

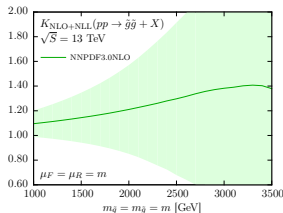
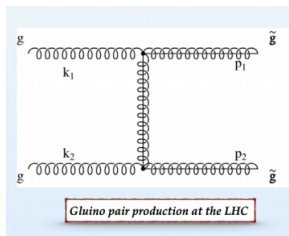


- PDFs will keep playing an important role for any future high energy collider involving hadrons in the initial state. Therefore improving our understanding of PDFs also strengthens the physics potential of such future colliders

 Gao, Harland-Lang, Rojo (2018)

PDF uncertainties and BSM Physics

The uncertainty on the PDFs is rapidly becoming one of the limiting factors in searches for new physics.



The relative size of the NLL corrections for gluino pair production was computed. The error in the relative size of the NLL corrections grows very quickly as the gluino mass is increased, mostly as a consequence of the large PDF errors at large values of x . [Beenakker et al. \(2016\)](#)

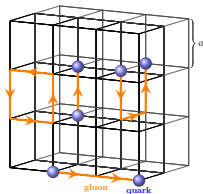
From DIS to PDFs via factorization

- The measurement of PDFs is made possible due to factorization theorems
- Intuitively, factorization theorems tell us that the same universal non-perturbative objects (the PDFs), representing long distance physics, can be combined with many short-distance calculations in QCD to give the cross-sections of various processes

$$\sigma = f \otimes H$$

- ▶ f are the PDFs, H is the hard perturbative part and \otimes is convolution.
- ▶ PDFs truly characterize the hadronic target
- ▶ PDFs are essentially non-perturbative

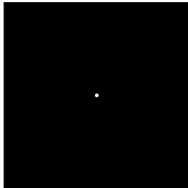
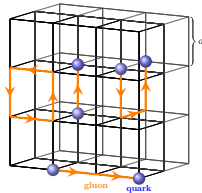
Lattice?



- The natural ab-initio method to study QCD non-perturbatively is on the lattice. But ...
- PDFs are defined as an expectation value of a bilocal operator evaluated along a light-like line.
- Clearly, we can not evaluate this on a Euclidean set-up.



Lattice?



- The natural ab-initio method to study QCD non-perturbatively is on the lattice. But ...
- PDFs are defined as an expectation value of a bilocal operator evaluated along a light-like line.
- Clearly, we can not evaluate this on a Euclidean set-up.

Lattice traditionally & global PDF fits

Light cone PDF

$$\hookrightarrow q(x) = \frac{1}{4\pi} \int_{-\infty}^{\infty} d\omega^- e^{-ixP^+\omega^-} \langle P | \bar{\psi}(\omega^-) W(\omega^-, 0) \gamma^+ \psi(0) | P \rangle$$

$$\text{where } W(\omega^-, 0) = \mathcal{P} e^{-ig_0 \int_0^{\omega^-} dy^- A^+(y^-)}$$

Lattice traditionally & global PDF fits

Light cone PDF

$$\hookrightarrow q(x) = \frac{1}{4\pi} \int_{-\infty}^{\infty} d\omega^- e^{-ixP^+\omega^-} \langle P | \bar{\psi}(\omega^-) W(\omega^-, 0) \gamma^+ \psi(0) | P \rangle$$

Mellin moments $\langle x^k \rangle_q = \int_{-1}^1 dx x^k q(x)$ related to local matrix elements of twist-2 operators

$$\langle P | \bar{\psi}(0) \gamma^{\{\mu_1} D^{\mu_2} \dots D^{\mu_k\}} \psi(0) | P \rangle = 2 \langle x^k \rangle_q (P^{\mu_1} \dots P^{\mu_k} - \text{traces})$$

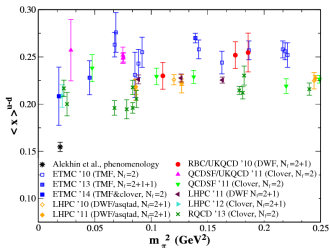
Lattice traditionally & global PDF fits

- Not an issue if every moment were accessible because a probability distribution is completely determined once all its moments are known.
 - These studies are limited to the first few (three) moments due to
 - ▶ Bad signal to noise ratio
 - ▶ Power-divergent mixing on the lattice (discretized space-time does not possess the full rotational symmetry of the continuum).
-

Lattice traditionally & global PDF fits

Mellin moments

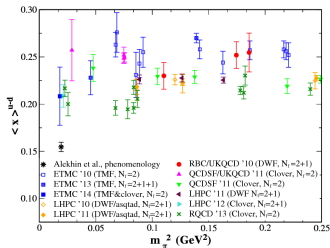
 Constantinou (2015)



Lattice traditionally & global PDF fits

Mellin moments

 Constantinou (2015)



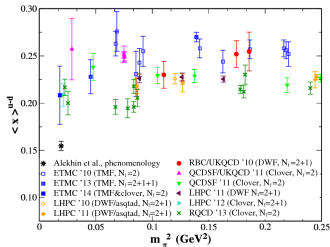
Global fits

- Usual determination of PDFs is performed by fitting experimental data from several hard scattering cross sections (l-p and p-p collisions)
- Combining the most PDF-sensitive data and the highest precision QCD and EW calculations (always assuming that SM holds) and employing a statistically robust fitting methodology
- Can achieve high precision for the cases that data are abundant

Lattice traditionally & global PDF fits

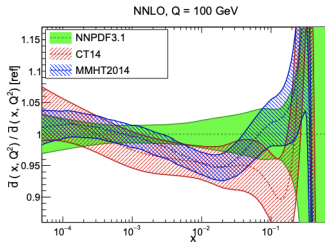
Mellin moments

Constantinou (2015)



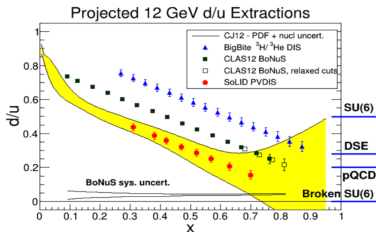
Global fits

Lin et al. (2018)



Large- x discrepancies for the nucleon and the pion

The nucleon



- JLab 12-GeV measurements of the ratio of the PDFs for the d and u quarks at large momentum fraction x
- In yellow the projected uncertainty in measurements under several theoretical assumptions

The pion

Model/theory	large x
QCD parton model	$(1-x)^2$
pQCD	$(1-x)^{2+\gamma}$
Light-front holographic QCD	$(1-x)^0$
Nambu-Jona-Lasino/duality	$(1-x)^1$

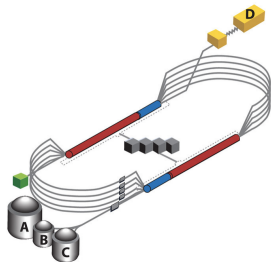
- \bar{u} quark distribution of π^- extracted @FNAL E615
- Large- x of pion PDF is the goal @JLab-C12-15-006, @COMPASS-CERN. Large- x of kaon PDF is the goal @JLab-C12-15-006A

An ab-initio non-perturbative QCD calculation is timely and imperative!

Experimental Research Facilities

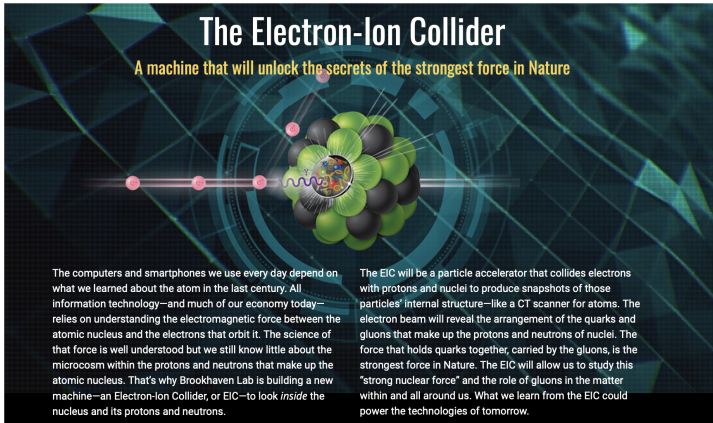


Experimental Research Facilities



JLAB 12 GeV upgrade

Experimental Research Facilities



The Electron-Ion Collider

A machine that will unlock the secrets of the strongest force in Nature

The computers and smartphones we use every day depend on what we learned about the atom in the last century. All information technology—and much of our economy today—relies on understanding the electromagnetic force between the atomic nucleus and the electrons that orbit it. The science of that force is well understood but we still know little about the microcosm within the protons and neutrons that make up the atomic nucleus. That's why Brookhaven Lab is building a new machine—an Electron-Ion Collider, or EIC—to look *inside* the nucleus and its protons and neutrons.

The EIC will be a particle accelerator that collides electrons with protons and nuclei to produce snapshots of those particles' internal structure—like a CT scanner for atoms. The electron beam will reveal the arrangement of the quarks and gluons that make up the protons and neutrons of nuclei. The force that holds quarks together, carried by the gluons, is the strongest force in Nature. The EIC will allow us to study this "strong nuclear force" and the role of gluons in the matter within and all around us. What we learn from the EIC could power the technologies of tomorrow.

taken from <https://www.bnl.gov/eic/>

The Ji Idea

- Lattice QCD computes equal time matrix elements
- Displace quarks in space-like interval
- Boost states to “infinite” momentum
- On the frame of the proton displacement becomes lightlike
- But infinite momentum not possible on the lattice
- Use perturbative matching from finite momentum [↗ X. Ji \(2013\)](#)
- One needs to deal with the divergences

PDFs from the lattice: Pseudo-PDFs Formalism

Starting point: the equal time hadronic matrix element with the quark and anti-quark fields separated by a finite distance [Radyushkin \(2017\)](#)

$$\mathcal{M}^\alpha(z, p) \equiv \langle p | \bar{\psi}(0) \gamma^\alpha \hat{E}(0, z; A) \tau_3 \psi(z) | p \rangle$$

$z = (0, 0, 0, z_3)$
 $p = (p^0, 0, 0, p)$
 $\alpha = 0$

Lorentz inv. \rightarrow

$$\mathcal{M}^\alpha(z, p) = 2p^\alpha \underbrace{\mathcal{M}_p(-(zp), -z^2)}_{\text{Leading twist}} + z^\alpha \underbrace{\mathcal{M}_z(-(zp), -z^2)}_{\text{Higher twist}}$$

- The Lorentz invariant quantity $\nu = -(zp)$, is the "loffe time"
- loffe time PDFs $\mathcal{M}(\nu, z_3^2)$ defined at a scale $\mu^2 = 4e^{-2\gamma_E}/z_3^2$ (at leading log level) are the Fourier transform of regular PDFs $f(x, \mu^2)$ [Balitsky, Braun \(1988\)](#), [Braun et al. \(1995\)](#)

$$\mathcal{M}(\nu, z_3^2) = \int_{-1}^1 dx f(x, 1/z_3^2) e^{i x \nu}$$

Formalism

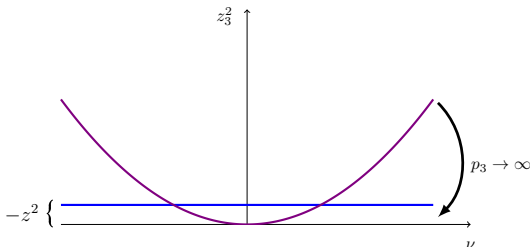
- The quasi-PDF $Q(x, p^2)$ is related to $\mathcal{M}_p(\nu, z_3^2)$ by

$$Q(x, p^2) = \frac{1}{2\pi} \int_{-\infty}^{\infty} d\nu e^{-ix\nu} \mathcal{M}_p(\nu, [\nu/p]^2)$$

Quasi PDF mixes invariant scales until p_z is effectively large enough

- While the pseudo-PDF has fixed invariant scale dependence

$$P(x, z_0^2) = \frac{1}{2\pi} \int_{-\infty}^{\infty} d\nu e^{-ix\nu} \mathcal{M}_p(\nu, z_0^2)$$



Lattice QCD requirements

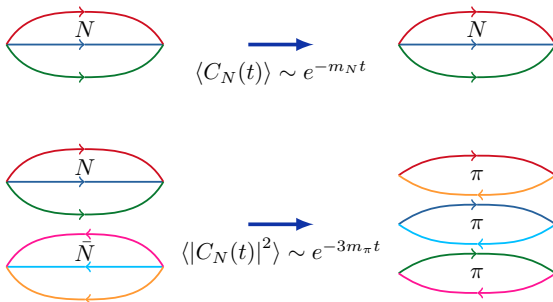
- Largest momentum on the lattice $aP_{max} = \pi/2 \propto \mathcal{O}(1)$
- $a = 0.1\text{fm} \rightarrow P_{max} = 10\Lambda$ where $\Lambda = 300 \text{ MeV}$
- $a = 0.05\text{fm} \rightarrow P_{max} = 20\Lambda$

Large momentum is required to suppress high twist effects (quasi-PDFs) and to provide a wide coverage of the loffe time ν

$P_{max} = 3 \text{ GeV}$ easily achievable with moderate values of the lattice spacing but still demanding due to statistical noise

$P_{max} = 6 \text{ GeV}$ exponentially harder requiring very fine values of the lattice spacing

Signal to Noise



Statistical accuracy drops exponentially with increasing momentum P


$$\text{StN}(O) = \frac{\langle O \rangle}{\sqrt{\text{var}(O)}} \propto e^{-[E_N(P) - 3/2m_\pi]t}$$

G. Parisi (1984) P. Lepage (1989) Statistical accuracy drops exponentially with the increasing momentum limiting the maximum achievable momentum.

Obtaining the Ioffe time PDF

$$z_3 \rightarrow 0 \Rightarrow \mathcal{M}_p(\nu, z_3^2) = \mathcal{M}(\nu, z_3^2) + \mathcal{O}(z_3^2)$$

But.... large $\mathcal{O}(z_3^2)$ corrections **prohibit** the extraction.

In a **ratio** z_3^2 corrections might cancel  Radyushkin (2017)

$$\mathfrak{M}(\nu, z_3^2) \equiv \frac{\mathcal{M}_p(\nu, z_3^2)}{\mathcal{M}_p(0, z_3^2)}$$

- Much **smaller** $\mathcal{O}(z_3^2)$ corrections and therefore this ratio could be used to extract the Ioffe time PDFs
- All UV singularities are **exactly cancelled** and when computed in lattice QCD it can be extrapolated to the continuum limit

■

$$\mathfrak{M}(\nu, z^2) = \int_0^1 d\alpha \mathcal{C}(\alpha, z^2 \mu^2, \alpha_s(\mu)) \mathcal{Q}(\alpha\nu, \mu) + \sum_{k=1}^{\infty} \mathcal{B}_k(\nu) (z^2)^k,$$

μ is the factorization scale and $\mathcal{Q}(\nu, \mu)$ is the Ioffe time PDF

Numerical implementation

First case study in an unphysical setup [Karpie, Orginos, Radyushkin SZ, Phys.Rev. D96 \(2017\) no.9, 094503](#)

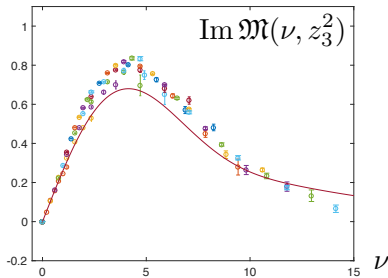
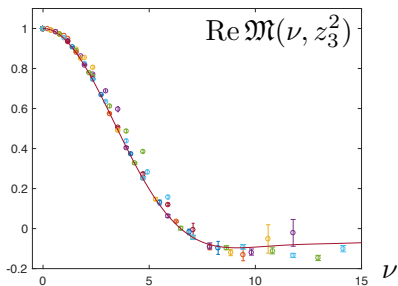
- Quenched approximation
- $32^3 \times 64$ lattices with $a = 0.093\text{fm}$.
- $m_\pi = 601\text{MeV}$ and $m_N = 1411\text{MeV}$

Now employing dynamical ensembles

$a(\text{fm})$	$M_\pi(\text{MeV})$	β	$L^3 \times T$
0.127(2)	440	6.1	$24^3 \times 64$
0.127(2)	440	6.1	$32^3 \times 96$
0.094(1)	400	6.3	$32^3 \times 64$
0.094(1)	280	6.3	$32^3 \times 64$
0.094(1)	172	6.3	$64^3 \times 128$

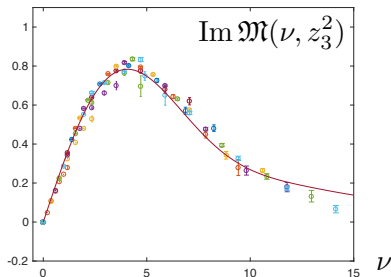
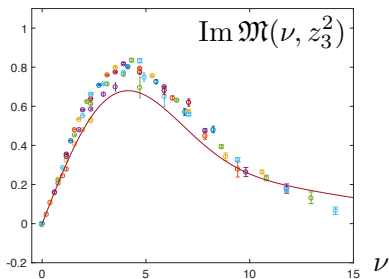
Table: Parameters for the lattices generated by the JLab/W&M collaboration using 2+1 flavors of clover Wilson fermions and a tree-level tadpole-improved Symanzik gauge action. The lattice spacings, a , are estimated using the Wilson flow scale w_0 . Stout smearing implemented in the fermion action makes the tadpole corrected tree-level clover coefficient c_{SW} used, to be very close to the value determined non-pertubatively with the Schrödinger functional method

Results for the Re and Im parts of $\mathfrak{M}(\nu, z_3^2)$



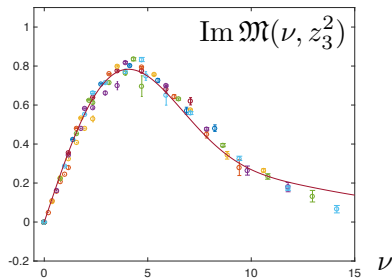
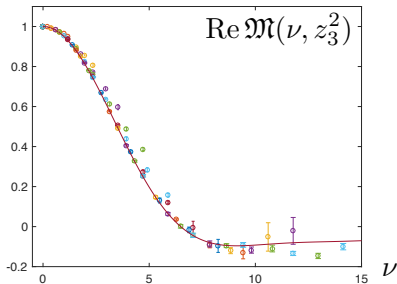
- Curves represent Re and Im Fourier transforms of $q_\nu(x) = \frac{315}{32} \sqrt{x}(1-x)^3$.
- Considering CP even and odd combinations
 - ▶ even: $q_-(x) = f(x) + f(-x) = q(x) - \bar{q}(x) = q_\nu(x)$
 - ▶ odd: $q_+(x) = f(x) - f(-x) = q(x) + \bar{q}(x) = q_\nu(x) + 2\bar{q}(x)$

Results for the Im part of $\mathfrak{M}(\nu, z_3^2)$



- Curves represent the Im Fourier transforms of $q_v(x) = q(x) - \bar{q}(x)$ and $q_+(x) = q(x) + \bar{q}(x) = q_v(x) + 2\bar{q}(x)$ respectively.
- The agreement with the data is strongly improved if we use a non-vanishing antiquark contribution, namely $\bar{q}(x) = \bar{u}(x) + \bar{d}(x) = 0.07[20x(1-x)^3]$.

Results for the Re and Im parts of $\mathfrak{M}(\nu, z_3^2)$



- Data as function of the loffe time. A **residual** z_3 -dependence can be seen.
- This is more visible when, for a **particular** ν we have several data points corresponding to **different values of** z_3 .
- Different values of z_3^2 for the same ν correspond to the loffe time distribution at different scales.

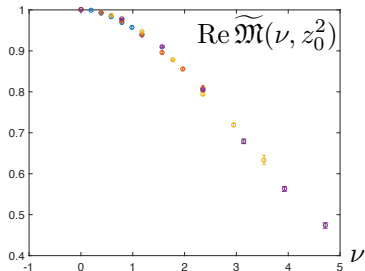
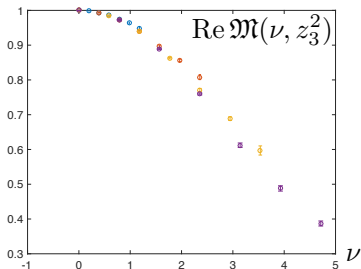
Residual z_3 -dependence

- Is the residual scatter in the data points **consistent with evolution**? By solving the evolution equation at LO, the loffe time PDF at z'_3 is related to the one at z_3 by

$$\mathfrak{M}(\nu, z'_3{}^2) = \mathfrak{M}(\nu, z_3^2) - \frac{2}{3} \frac{\alpha_s}{\pi} \ln(z'_3{}^2/z_3^2) \int_0^1 du B(u) \mathfrak{M}(u\nu, z_3^2)$$

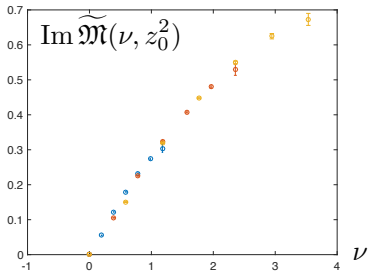
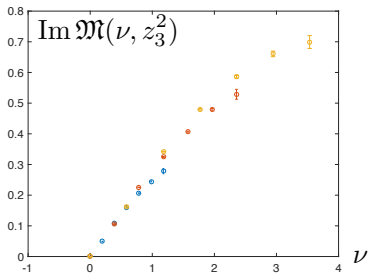
- Only applicable at small z_3
- Check its effect using data at values of $z_3 \leq 4a$ corresponding to energy scales larger than 500 MeV.
- We fix the point z'_3 at the value $z_0 = 2a$ corresponding, at leading logarithm level, to the $\overline{\text{MS}}$ -scheme scale $\mu_0 = 1$ GeV and evolve the rest of the points to that scale.

Before and after evolution



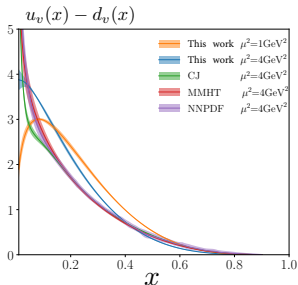
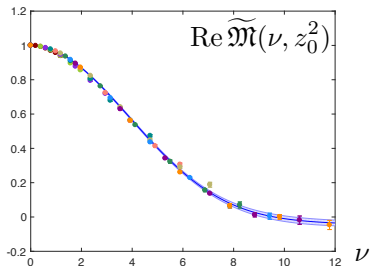
The ratio $\mathfrak{M}(\nu, z_3^2)$ for $z_3/a = 1, 2, 3,$ and 4 . **LHS:** Data before evolution. **RHS:** Data after evolution. The reduction in scatter indicates that evolution collapses all data to the same universal curve.

Before and after evolution



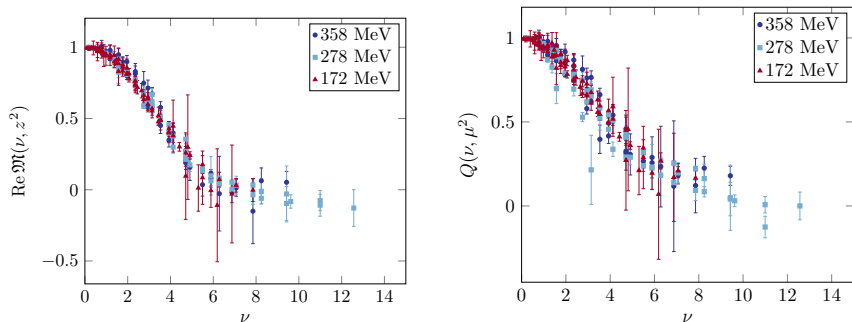
The ratio $\mathfrak{M}(\nu, z_3^2)$ for $z_3/a = 1, 2, 3, \text{ and } 4$. **LHS:** Data before evolution. **RHS:** Data after evolution. The reduction in scatter indicates that evolution collapses all data to the same universal curve.

Comparisons with global fits



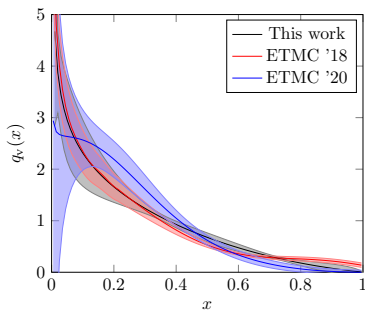
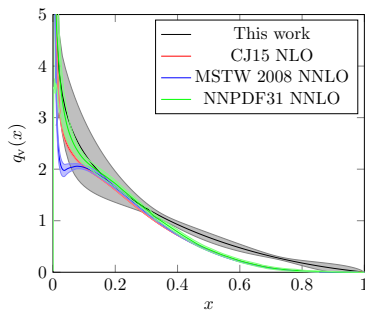
Left: Data points for $\text{Re } \widetilde{\mathfrak{M}}(\nu, z_3^2)$ with $z_3 \leq 10a$ evolved to $z_3 = 2a$ as described in the text. Right: Curve for $u_v(x) - d_v(x)$ built from the evolved data shown in the left panel and treated as corresponding to the $\mu^2 = 1 \text{ GeV}^2$ scale; then evolved to the reference point $\mu^2 = 4 \text{ GeV}^2$ of the global fits.

Numerical Results



The real part of the reduced pseudo-ITD calculated on ensembles with 358 MeV, 278 MeV, and 172 MeV pion masses (LHS) and the corresponding \overline{MS} ITD at 2 GeV (RHS) [Joo, Karpie, Orginos, Radyushkin, Richards, S.Z. Phys.Rev.Lett. 125 \(2020\) 23, 232003](#)

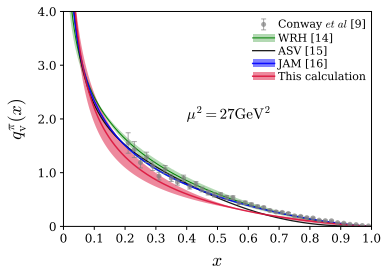
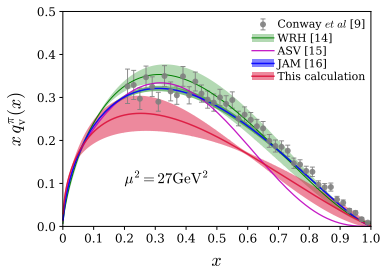
New results with $N_f = 2 + 1$ fermions for the nucleon



Our determination of the phys. pion mass nucleon valence PDF compared to pheno and other lattice determinations. [🔗 Joo, Karpie, Orginos, Radyushkin, Richards, S.Z.](#)

[Phys.Rev.Lett. 125 \(2020\) 23, 232003](#)

Results with $N_f = 2 + 1$ flavors for the pion



(LHS) Comparison of the pion $xq_V^\pi(x)$ -distribution with the LO extraction from DY data (gray data points), NLO fits (green, maroon, and blue). This lattice QCD calculation of $q_V^\pi(x)$ is evolved from an initial scale $\mu_0^2 = 4 \text{ GeV}^2$ at NLO. All the results are evolved to an evolution scale of $\mu^2 = 27 \text{ GeV}^2$. Similar comparison of the pion $q_V^\pi(x)$ -distribution (RHS). [Joo, Karpie, Orginos, Radyushkin, Richards, Sufian S.Z. Phys.Rev.D 100 \(2019\) 11, 114512](#)

[Radyushkin, Richards, Sufian S.Z. Phys.Rev.D 100 \(2019\) 11, 114512](#)

The pertinent systematics in PDF extraction


- Parton distribution functions or distribution amplitudes may be defined in lattice QCD by inverting the quasi-Fourier transform of a certain class of hadronic position-space matrix elements
- One example are the Ioffe-time PDFs, \mathfrak{M}_R , related to the physical PDF $q_v(x, \mu^2)$ via the integral relation

$$\mathfrak{M}_R(\nu, \mu^2) \equiv \int_0^1 dx \cos(\nu x) q_v(x, \mu^2)$$

The pertinent systematics in PDF extraction

- Parton distribution functions or distribution amplitudes may be defined in lattice QCD by inverting the quasi-Fourier transform of a certain class of hadronic position-space matrix elements
- One example are the Ioffe-time PDFs, \mathfrak{M}_R , related to the physical PDF $q_v(x, \mu^2)$ via the integral relation

Only a handful
of lattice data


$$\mathfrak{M}_R(\nu, \mu^2) \equiv \int_0^1 dx \cos(\nu x) q_v(x, \mu^2)$$

 Karpie, Orginos, Rothkopf, S.Z. JHEP 1904 (2019) 057

The pertinent systematics in PDF extraction

- Parton distribution functions or distribution amplitudes may be defined in lattice QCD by inverting the quasi-Fourier transform of a certain class of hadronic position-space matrix elements
- One example are the Ioffe-time PDFs, \mathfrak{M}_R , related to the physical PDF $q_v(x, \mu^2)$ via the integral relation

Only a handful
of lattice data

$$\mathfrak{M}_R(\nu, \mu^2) \equiv \int_0^1 dx \cos(\nu x) q_v(x, \mu^2)$$

Cosine not orthogonal in $[0, 1]$

The pertinent systematics in PDF extraction

- Parton distribution functions or distribution amplitudes may be defined in lattice QCD by inverting the quasi-Fourier transform of a certain class of hadronic position-space matrix elements
- One example are the Ioffe-time PDFs, \mathfrak{M}_R , related to the physical PDF $q_v(x, \mu^2)$ via the integral relation

Only a handful
of lattice data

$$\mathfrak{M}_R(\nu, \mu^2) \equiv \int_0^1 dx \cos(\nu x) q_v(x, \mu^2)$$

Cosine not orthogonal in $[0, 1]$

- The task at hand is then to **reconstruct the PDF $q_v(x, \mu^2)$ given a limited set of simulated data** for $\mathfrak{M}_R(\nu, \mu^2)$.
- The extraction is highly ill-posed, so one has to resort to regularization strategies in order to find a way to reliably estimate the PDF from the data at hand

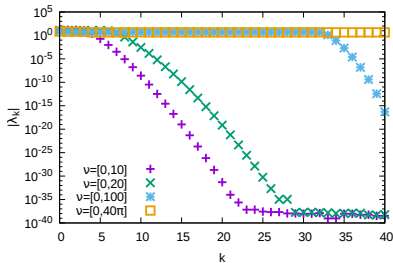
 Karpie, Orginos, Rothkopf, S.Z. JHEP 1904 (2019) 057

Naive Reconstruction

- Discretize the integral, employing the trapezoid rule

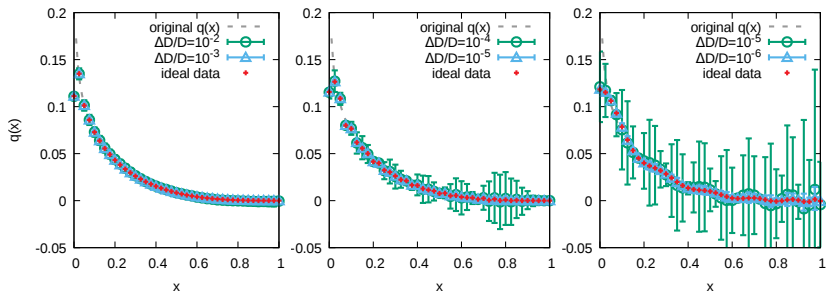
$$\mathfrak{M}_R(\nu) = \frac{1}{2} \cos(\nu x_0) q_v(x_0) + \sum_{k=1}^{N_x-1} \delta x \cos(\nu x_k) q_v(x_k) + \frac{1}{2} \cos(\nu x_{N_x}) q_v(x_{N_x})$$

- Casting our problem in a matrix equation $\mathfrak{m} = \mathfrak{C} \cdot \mathfrak{q}$,
- The conditioning of the problem is easily elucidated by considering the eigenvalues of the matrix \mathfrak{C} .



 Karpie, Orginos, Rothkopf, S.Z. - arXiv:1901.05408 - JHEP 1904 (2019) 057

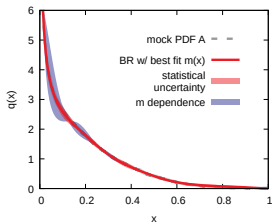
Naive Reconstruction



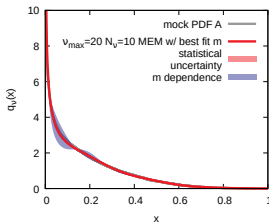
Results for the direct inversion for different discretization intervals (left $\nu = [0, 40\pi]$, center $\nu = [0, 100]$, right $\nu = [0, 20]$). Note the different size of the relative errors needed, to obtain a well behaved result (left $\Delta\mathfrak{M}_R/\mathfrak{M}_R = 10^{-2}$, center $\Delta\mathfrak{M}_R/\mathfrak{M}_R = 10^{-5}$, right $\Delta\mathfrak{M}_R/\mathfrak{M}_R = 10^{-6}$).

Advanced PDF Reconstructions

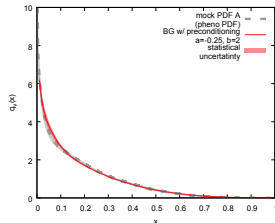
Bayesian Reconstruction



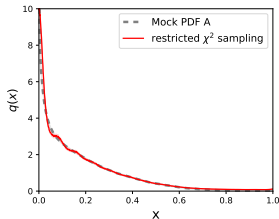
Max. Entropy Method



Backus-Gilbert algorithm

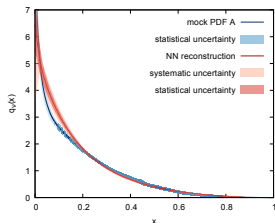


HMC χ^2 evaluation



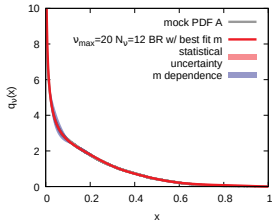
- Bayesian Reconstruction
- Max. Entropy Method
- Backus-Gilbert algorithm
- HMC χ^2 evaluation
- Neural Network

Neural Network

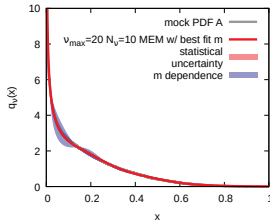


Advanced PDF Reconstructions

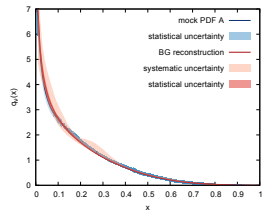
Bayesian Reconstruction



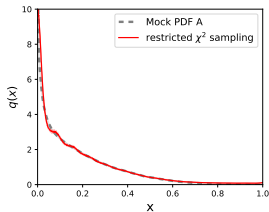
Max. Entropy Method



Backus-Gilbert algorithm

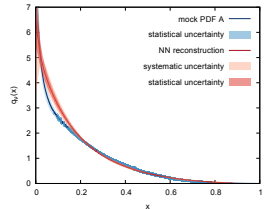


HMC χ^2 evaluation



Capitalize of the good scanning in loffe time and use advanced reconstruction methods to extract the maximum amount of information also for the small- x region.

Neural Network



 Karpie, Orginos, Rothkopf, S.Z. JHEP 1904 (2019) 057

Global fitting lattice data in the NNPDF framework

Focus on lattice observables, ie. a quantity which can be computed on the lattice on one hand, and related to some collinear PDFs through some kind of factorization theorem on the other. We consider the case of the unpolarized isovector parton distribution the definition of the two nonsinglet PDFs V_3 and T_3

$$V_3(x) = u(x) - \bar{u}(x) - [d(x) - \bar{d}(x)],$$
$$T_3(x) = u(x) - \bar{u}(x) + [d(x) - \bar{d}(x)],$$

we can define the two lattice observables

$$\text{Re}[\mathfrak{M}](\nu, -z_3^2) = \int_0^1 dx C^{\text{Re}}(x\nu, \mu^2 z_3^2) V_3(x, \mu^2),$$
$$\text{Im}[\mathfrak{M}](\nu, -z_3^2) = \int_0^1 dx C^{\text{Im}}(x\nu, \mu^2 z_3^2) T_3(x, \mu^2),$$

Global fitting lattice data in the NNPDF framework

with

$$C^{\text{Re}} = \cos(\xi) - \frac{\alpha_s}{2\pi} C_F \int_0^1 dw \left[B(w) \log\left(z_3^2 \mu^2 \frac{e^{2\gamma_E+1}}{4}\right) + L(w) \right] \cos(\xi w),$$
$$C^{\text{Im}} = \sin(\xi) - \frac{\alpha_s}{2\pi} C_F \int_0^1 dw \left[B(w) \log\left(z_3^2 \mu^2 \frac{e^{2\gamma_E+1}}{4}\right) + L(w) \right] \sin(\xi w)$$

where the kernels $B(w)$ and $L(w)$, are given by

$$B(w) = \left[\frac{1+w^2}{1-w} \right]_+$$
$$L(w) = \left[4 \frac{\log(1-w)}{1-w} - 2(1-w) \right]_+.$$

Global fitting lattice data in the NNPDF framework

- Given a set of lattice data for the real and imaginary part of the reduced pseudo-ITD, the distributions T_3 and V_3 can be extracted from them through a standard χ^2 fit
- where the unknown x -dependence of the PDFs is parameterized at the chosen scale μ^2
- using a suitable parametric form, whose best parameters are determined minimizing the χ^2
- Using the NNPDF fitting framework, running the same machinery commonly used to extract PDFs from experimental data.
- x -dependence of $f_q(x)$ parameterized through a neural network NN_q multiplied by a preprocessing polynomial factor

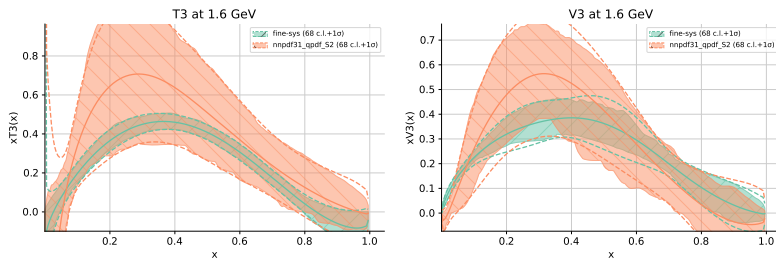
$$f_q(x) = x^{\alpha_q} (1-x)^{\beta_q} \text{NN}_q(x),$$

α_q, β_q being additional free parameters determined by the fit

Global fitting lattice data in the NNPDF framework

- NNPDF methodology has been used to produce PDF sets for years
- provides a flexible environment
- possible to fit more than 4000 experimental points
- from a variety of different high energy processes in different kinematic ranges. NNPDF collaboration R. Ball et al, Eur.Phys.J.C 77 (2017) 10, 663, JHEP 04 (2015) 040
- reliable framework used to study and analyze the available lattice data
- to assess how well these are able to constrain the PDFs
- to compare lattice results with those coming from standard PDF sets.
- important to emphasize once again that in this analysis, once the FastKernel tables have been generated, the lattice data are treated exactly on the same footing as any other data
- viz. the exact same methodology and code are used for fitting experimental and lattice data.

Global fitting lattice data in the NNPDF framework



Quasi-PDFs and pseudo-ITD results are plotted together. Both T3 and V3 distributions appear to be in good agreement, the main difference being a huge decrease in the PDFs error when considering results presented in this work. [🔗 Del Debbio, Giani, Karpie, Orginos, Radyushkin, S.Z. JHEP 02 \(2021\) 138](#) [🔗 Cichy, Del Debbio, Giani JHEP 10 \(2019\) 137](#)

Lessons from a comparison of quasi and pseudo data implemented in the NNPDF framework

Comparison between our results *fine-sys* with the best result of [K. Cichy, L. Del Debbio and T. Giani, JHEP 10 \(2019\) 137](#). Both PDFs sets have been obtained using the same NNPDF methodology, the only difference being the input data (pseudo-ITD and quasi-PDFs data respectively) and the corresponding errors.

- Good agreement between the distributions
- huge decrease in the PDFs error from the pseudo-framework
- partially traced back to the number of points included in the analysis
- 16 points for quasi-PDFs matrix element compared to data corresponding to all momenta, for a total of 48 pseudo-ITD points.
- More points in the analysis allow to better constraint the fits, giving final PDFs with smaller error.
- Equivalent computational cost, the low momenta matrix elements, (used by the pseudo approach), are exponentially more precise than the large momenta matrix elements, (restriction for the quasi approach).

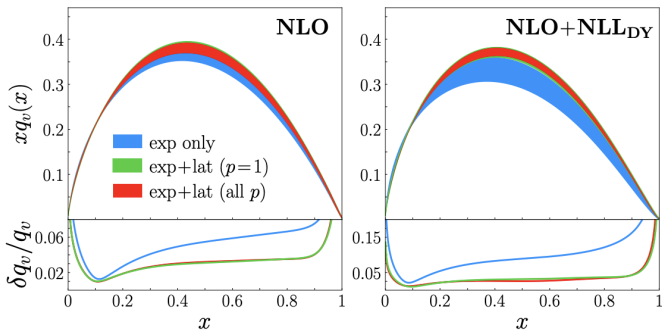
Global fitting lattice data in the NNPDF framework

Lattice ensemble	$a(\text{fm})$	M_π (MeV)	$L^3 \times T$	n_{dat}
fine	0.094(1)	358(3)	$32^3 \times 64$	48
big	0.127(2)	415(23)	$32^3 \times 96$	48
coarse	0.127(2)	415(23)	$24^3 \times 64$	36
280	0.094(1)	278(3)	$32^3 \times 64$	64
170	0.091(1)	172(6)	$64^3 \times 128$	80

The lattice ensembles used for the NNPDF reco of the lattice data [🔗 Del Debbio,](#)

[Giani, Karpie, Orginos, Radyushkin, S.Z. JHEP 02 \(2021\) 138](#)

Complementarity of experimental and lattice QCD data on pion parton distributions



Valence quark distributions (**top**) when extracted from experimental data alone (blue), combined with the $p = 1$ lattice data (green), and combined with all the lattice data (red) for the NLO (**left**) and NLO+NLL_{DY} (**right**) cases, along with the relative uncertainties (**bottom**). The bands represent a 1σ uncertainty level. [Barry, Egerer, Karpie, Melnitchouk, Orginos, Richards, Sato, Sufian, Qiu, S.Z.](#)

Phys.Rev.D 105 (2022) 11, 114051

The Continuum and Leading Twist Limits of Parton Distribution Functions in Lattice QCD

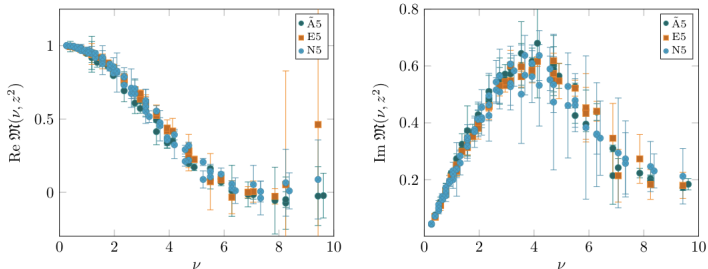
- In [Karpie, Orginos, Radyushkin and S.Z. JHEP 11 \(2021\) 024](#) we present continuum limit results
- first continuum limit using the pseudo-PDF approach with Short Distance Factorization for factorizing lattice QCD calculable matrix elements
- we are employing the summation Generalized Eigenvalue Problem (sGEVP) technique in order to optimize our control over the excited state contamination which can be one of the most serious systematic errors in this type of calculations
- crucial novel ingredient of our analysis is the parameterization of systematic errors using Jacobi polynomials to characterize and remove both lattice spacing and higher twist contaminations, as well as the leading twist distribution
- method can be expanded in further studies to remove all other systematic errors

The Continuum and Leading Twist Limits of Parton Distribution Functions in Lattice QCD

ID	$a(\text{fm})$	$M_\pi(\text{MeV})$	β	c_{SW}	κ	$L^3 \times T$	N_{cfg}
$\tilde{A}5$	0.0749(8)	446(1)	5.2	2.01715	0.13585	$32^3 \times 64$	1904
E5	0.0652(6)	440(5)	5.3	1.90952	0.13625	$32^3 \times 64$	999
N5	0.0483(4)	443(4)	5.5	1.75150	0.13660	$48^3 \times 96$	477

Parameters for the lattices generated by the CLS collaboration using two flavors of $\mathcal{O}(a)$ improved Wilson fermions.

The Continuum and Leading Twist Limits of Parton Distribution Functions in Lattice QCD



The real (LHS) and the imaginary (RHS) part of the reduced ITDs of the three lattice ensembles used in this study. We see that for the range of loffe times that is covered by our data the three ensembles have a pretty good overlap. The statistical and systematic errors are added in quadrature.

The Continuum and Leading Twist Limits of PDFs

- The continuum limit is a critical step in any precision lattice calculation.
- Take advantage of the symmetries of the reduced pseudo-ITD to parameterize the lattice spacing and the higher twist effects.
- The continuum PDF is also parameterized and a simultaneous analysis of all three ensembles obtains the continuum limit PDF with higher twist contamination removed.
- This method of adding “nuisance parameters” to parameterize the systematic errors of experimental cross sections is also used in the pheno extractions of PDFs.
- Generalize this to combine different pion masses, lattice spacings, matrix elements, lattice actions given appropriate parameterizations.
- Utilize all published results and analyzing them, given sufficiently novel nuisance parameterizations, just as a global phenomenological fit is performed using experimental data with vastly different systematic errors (here we correct for discretization errors and higher twist).

The Continuum and Leading Twist Limits of Parton Distribution Functions in Lattice QCD

A Taylor expansion in lattice spacing gives the continuum reduced pseudo-ITD $\mathfrak{M}_{\text{cont}}$ and lattice spacing corrections

$$\mathfrak{M}(p, z, a) = \mathfrak{M}_{\text{cont}}(\nu, z^2) + \sum_{n=1} \left(\frac{a}{|z|} \right)^n P_n(\nu) + (a\Lambda_{\text{QCD}})^n R_n(\nu)$$

With an $O(a)$ improved lattice action, the lattice spacing errors related to the momentum p , must come in from the momentum transfer. This feature is known in the improvement of the local vector current. The higher twist power corrections are added as nuisance terms similar to the lattice spacing terms. The functional form is given by

$$\mathfrak{M}_{\text{cont}}(\nu, z^2) = \mathfrak{M}_{\text{lt}}(\nu, z^2) + \sum_{n=1} (z^2 \Lambda_{\text{QCD}}^2)^n B_n(\nu).$$

The Continuum and Leading Twist Limits of Parton Distribution Functions in Lattice QCD

All of the unknown functions, $q_-(x)$, $q_+(x)$, $P_1(\nu)$, $R_1(\nu)$, and $B_1(\nu)$, are parameterized using Jacobi polynomials.

The Jacobi polynomials, $j_n^{(\alpha,\beta)}(z)$, are defined in the interval $[-1, 1]$ and they satisfy the orthogonality relation

$$\int_{-1}^1 dz (1-z)^\alpha (1+z)^\beta j_n^{(\alpha,\beta)}(z) j_m^{(\alpha,\beta)}(z) = \tilde{N}_n^{(\alpha,\beta)} \delta_{n,m},$$

for $\alpha, \beta > -1$. COV $x = \frac{1-z}{2}$ or $z = 1 - 2x$. This transformation maps the interval $[-1, 1]$ to the interval $[0, 1]$ and the orthogonality weight becomes $(1-z)^\alpha (1+z)^\beta = 2^{\alpha+\beta} x^\alpha (1-x)^\beta$. We then introduce the transformed Jacobi polynomials $J_n^{(\alpha,\beta)}(x)$, as

$$J_n^{(\alpha,\beta)}(x) = \sum_{j=0}^n \omega_{n,j}^{(\alpha,\beta)} x^j.$$

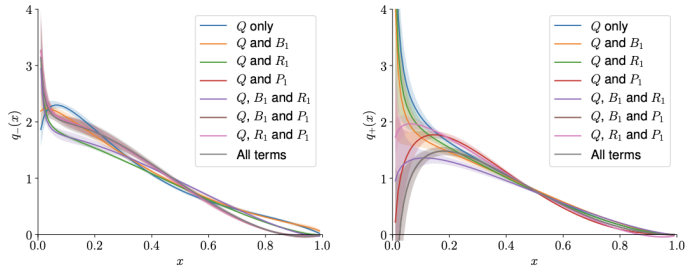
The Continuum and Leading Twist Limits of PDFs

Since the Jacobi polynomials form a complete basis of functions in the interval of $[0,1]$, the PDFs can be written as

$$q_{\pm}(x) = x^{\alpha}(1-x)^{\beta} \sum_{n=0}^{\infty} \pm d_n^{(\alpha,\beta)} J_n^{(\alpha,\beta)}(x)$$

for any α and β . The choice of those parameters does affect the convergence of the coefficients $\pm d_n^{(\alpha,\beta)}$. One needs to truncate the series introducing in this way some model dependence which can be easily controlled. The control of the truncation can be improved if one fits for the optimal values of α and β for that given order of truncation. In other words, the rate of convergence of the series can be optimized by tuning the values of α and β .

The Continuum and Leading Twist Limits of PDFs



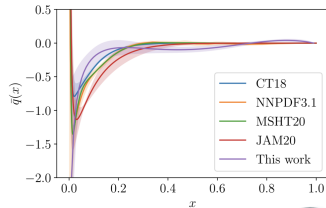
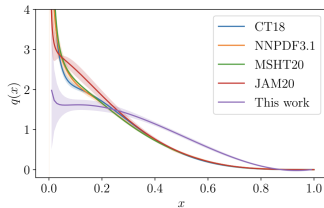
The results of fitting with various nuisance terms included.

The Continuum and Leading Twist Limits of PDFs

model	Real L^2 /d.o.f.	Real χ^2 /d.o.f.	Imag L^2 /d.o.f.	Imag χ^2 /d.o.f.
Q only	3.173	3.094	3.146	3.095
Q and B_1	2.721	2.479	3.054	2.969
Q and R_1	3.028	2.748	3.068	2.871
Q and P_1	0.876	0.809	1.186	1.088
Q , B_1 , and R_1	2.610	2.057	2.917	2.619
Q , B_1 , and P_1	0.852	0.723	1.020	0.888
Q , R_1 , and P_1	0.881	0.763	1.289	1.063
All terms	0.857	0.727	1.026	0.893

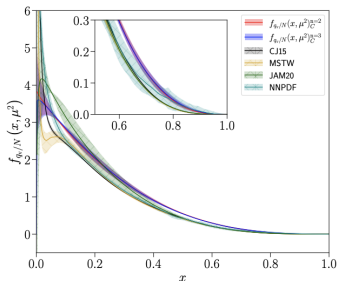
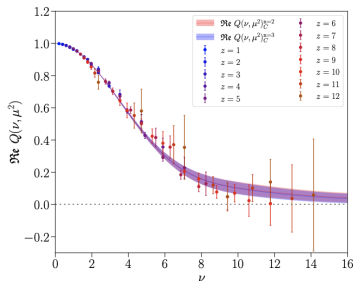
The L^2 /d.o.f. and χ^2 /d.o.f. of models using 2 Jacobi polynomials for the PDF and 1 Jacobi polynomial for the various nuisance terms from fits to the real and imaginary components of the reduced pseudo-ITD. The change in the L^2 /d.o.f. is a metric to judge the necessity of various nuisance terms. The most dramatic decreases occur when $O(\frac{a}{z})$ nuisance terms are included.

The Continuum and Leading Twist Limits of PDFs



Isvector quark and anti-quark distributions-comparing to phenomenology

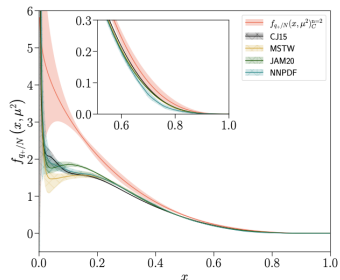
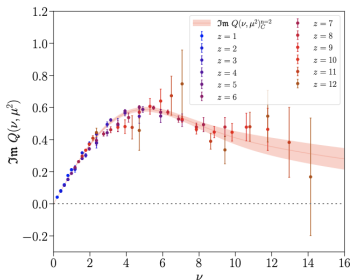
Towards High-Precision Parton Distributions From Lattice QCD via Distillation



The real component of the matched ITD at $\mu = 2$ GeV in $\overline{\text{MS}}$ fit by cosine transforms of two- and three-parameter model PDFs. The nucleon unpolarized valence quark PDF at 2 GeV in $\overline{\text{MS}}$ determined from the uncorrelated cosine transform fits applied to real component of the matched ITD. Comparisons are made with the NLO global analyses of CJ15 and JAM20, and the NNLO analyses of MSTW and NNPDF at the same scale.

 Egerer, Edwards, Kallidonis, Orginos, Radyushkin, Richards, Romero and S.Z. JHEP11(2021)148

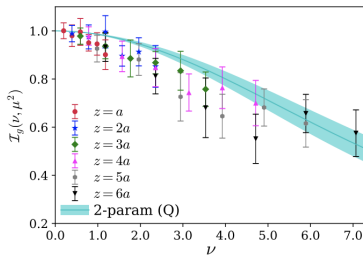
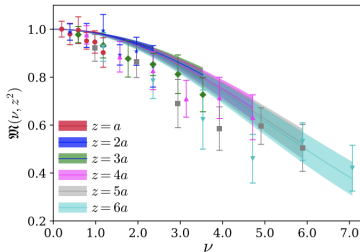
Towards High-Precision Parton Distributions From Lattice QCD via Distillation




The imaginary component of the matched ITD at $\mu = 2$ GeV in $\overline{\text{MS}}$ fit by the sine transform of a two-parameter model PDF. Data has been fit for $z/a \leq 12$, and correlations have been neglected. The nucleon unpolarized plus quark PDF at 2 GeV in $\overline{\text{MS}}$ determined from the uncorrelated sine transform fits applied to the imaginary component of the matched ITD. Comparisons are made with the NLO global analyses of CJ15 and JAM20, and the NNLO analyses of MSTW and NNPDF at the same scale. [Egerer,](#)

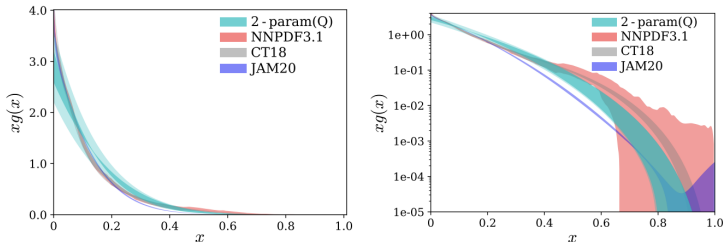
[Edwards, Kallidonis, Orginos, Radyushkin, Richards, Romero and S.Z. JHEP11\(2021\)148](#)

Gluon PDF



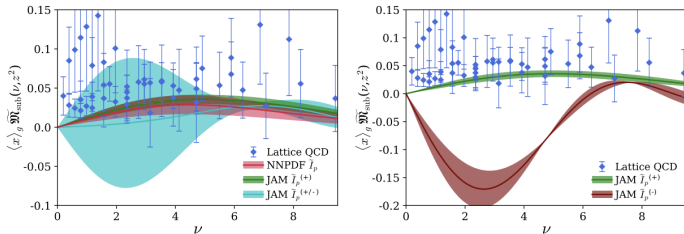
 Khan, Sufian, Karpie, Monahan, Egerer, Joo, Morris, Orginos, Radyushkin, Richards, Romero and S.Z. *Phys.Rev.D* 104 (2021) 9, 094516 Lattice reduced pseudo-ITD shown along with their reconstructed fitted bands and the $\overline{\text{MS}}$ matched ITD at 2GeV.


Gluon PDF



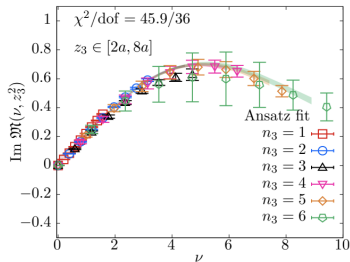
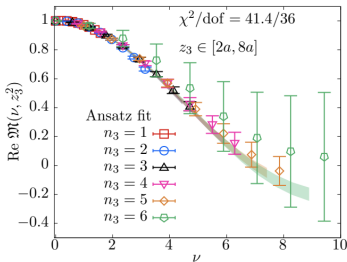
[Khan, Sufian, Karpie, Monahan, Egerer, Joo, Morris, Orginos, Radyushkin, Richards, Romero and S.Z. Phys.Rev.D 104 \(2021\) 9, 094516](#) Unpolarized gluon PDF (cyan band) extracted from our lattice data using the 2-param (Q) model. We compare our results to gluon PDFs extracted from global fits to experimental data, CT18, NNPDF3.1, and JAM20. Normalization of the gluon PDF using the gluon momentum fraction $\langle x \rangle_g^{\overline{MS}}(\mu = 2 \text{ GeV}) = 0.427(92)$ from [Alexandrou et al Phys.Rev.D 101 \(2020\) 9, 094513](#). On the L/RHS the same distributions with different scales for $xg(x)$ to enhance the view of the large- x region.


Gluon helicity distribution



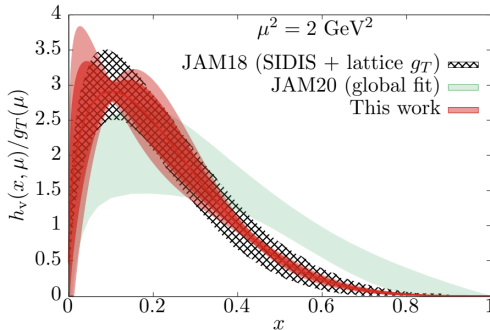
 Egerer, Joo, Karpie, Karthik, Khan, Monahan, Morris, Orginos, Radyushkin, Richards, Romero, Sufian and S.Z, *Phys.Rev.D* 106 (2022) 9, 094511 The lattice reduced pITD in the zero flow-time limit obtained through the subtraction method using the $p = 0$ matrix elements, and the gluon helicity ITD constructed from global fits. In the LHS the red band denotes the ITD constructed from the gluon helicity distribution by the NNPDF collaboration. The green band and the cyan band represent the gluon helicity ITD determined by the JAM collaboration with and without the positivity constraint. The green band and the maroon band represent the gluon helicity ITD determined by the JAM collaboration associated with the positive and negative gluon helicity PDF solutions.

Transversity PDF



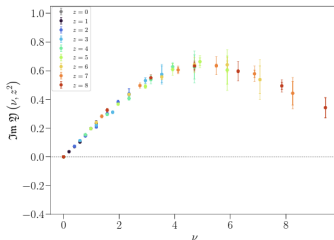
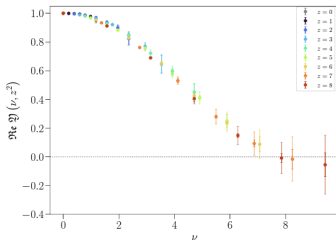
 Egerer, Kallidonis, Karpie, Karthik, Morris, Orginos, Radyushkin, Romero, Sufian and S.Z. *Phys.Rev.D* 105 (2022) 3, 034507 Reconstruction of transversity PDF based on a “Jam Ansatz”. The real and imaginary parts of \mathfrak{M} are shown as a function of ν . They show the best fit bands resulting from an analysis assuming the PDF ansatz. The fits shown in the figure incorporated the data points at all momenta with $z_3 \in [2a, 8a]$. The color of the bands and the data points distinguish the fixed value of momenta $P_3 = 0.41n_3$ GeV used.


Transversity PDF



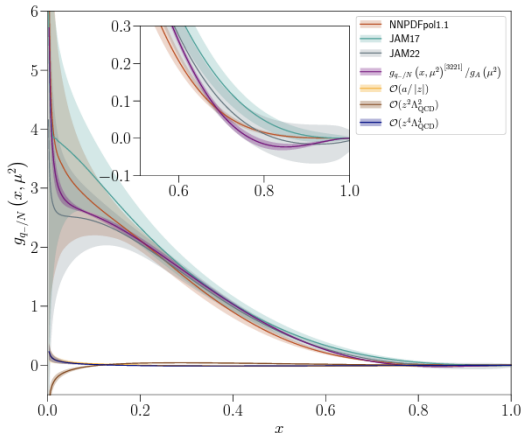
[Egerer, Kallidonis, Karpie, Karthik, Morris, Orginos, Radyushkin, Romero, Sufian and S.Z. Phys.Rev.D 105 \(2022\) 3, 034507](#) The valence transversity distribution $h_v(x, \mu)/g_T(\mu)$. The inner red band includes only the statistical error and the outer red band includes statistical and systematical errors in the PDF reconstruction. Comparison is made with the previous phenomenological determinations using SIDIS and lattice g_T (JAM18), shown using a patterned band, and with the recently updated global fit analysis (JAM20) of the single transverse spin asymmetry data (but, without including lattice g_T), shown as a green band.


Helicity PDF



 Egerer, Kallidonis, Karpie, Karthik, Morris, Orginos, Radyushkin, Romero, Sufian and S.Z. Phys.Rev.D 105 (2022) 3, 034507 Real and Imaginary components of the reduced pseudo-ITD

Helicity PDF



 Edwards, Egerer, Karpie, Karthik, Morris, Orginos, Radyushkin, Romero, Sufian and S.Z. Phys.Rev.D 105 (2022) 3, 034507 The leading-twist valence helicity quark PDF (purple) and x -space contaminations compared with the recent global analyses

Conclusions and outlook

- PDFs are needed as theoretical inputs to all hadron scattering experiments and in some cases are the largest theory uncertainty.
- The lattice community is by now able to provide ab-initio determinations of PDFs without theoretical obstructions.
- The interplay between lattice QCD and global fits is very important
- Also important in the search of New Physics [Gao, Harland-Lang, Rojo \(2018\)](#)
- What next?
- **Many thanks for your attention!!!**